INTERNATIONAL JOURNAL OF
NUMERICAL ANALYSIS AND MODELING
Volume 5, Number 2, Pages 331–351

OPTIMAL DESIGN OF THE SUPPORT OF THE CONTROL FOR THE 2-D WAVE EQUATION: A NUMERICAL METHOD

ARNAUD MÜNCH

Abstract. We consider in this paper the homogeneous 2-D wave equation defined on $\Omega \subset \mathbb{R}^2$. Using the Hilbert Uniqueness Method, one may associate to a suitable fixed subset $\omega \subset \Omega$, the control v_ω of minimal $L^2(\omega \times (0,T))$-norm which drives to rest the system at a time $T > 0$ large enough. We address the question of the optimal position of ω which minimize the functional $J : \omega \to ||v_\omega||_{L^2(\omega\times(0,T))}$. Assuming $\omega \in C^1(\Omega)$, we express the shape derivative of J as a curvilinear integral on $\partial\omega \times (0,T)$ independently of any adjoint solution. This expression leads to a descent direction and permits to define a gradient algorithm efficiently initialized by the topological derivative associated to J. The numerical approximation of the problem is discussed and numerical experiments are presented in the framework of the level set approach. We also investigate the well-posedness of the problem by considering its relaxation.

Key Words. Optimal shape design, Exact controllability of wave equation, Level set method, Numerical schemes, Relaxation.

1. Introduction - Problem statement

We consider in this work a general optimal design problem in the context of the (exact) controllability. There is by now a large interest in optimal shape design theory [9, 14], specially for dynamical system [13, 24], which consists in optimizing the distributions of materials or the shape of a mechanical structure in order to reach a suitable optimal behavior with respect to some initial excitation. On the other hand, since twenty years, a huge literature in the field of control has been devoted to the modeling and the analysis of mechanical systems, stabilized or exactly controlled in time, by some boundary or internal dissipative mechanisms [16, 17, 18, 19]. For instance, we mention the example of a multi-layered composite plate locally controlled by some piezo-electric device [15]. In order to extend this optimization process, it appears natural to optimize the shape and design of such dissipative mechanisms, distributed on the structure. We treat here this question in the context of the 2-D wave equation with an internal control. To the knowledge of the author, the coupling of these two notions - shape optimal design and exact controllability - has not been addressed so far.

Let us consider a Lipschitzian bounded domain $\Omega \in \mathbb{R}^2$, two functions $(y^0, y^1) \in H_0^1(\Omega) \times L^2(\Omega)$ and a real $T > 0$. In the context of the exact distributed controllability, one may determine a subset ω of positive Lebesgue measure for which the following property holds (see [3, 12, 19]) : there exists a control function $v_\omega \in$

Received by the editors May 2, 2006 and, in revised form, April 15, 2007.
2000 *Mathematics Subject Classification.* 35L05, 49J20, 65K10, 65M60, 93B05.

$L^2(\omega\times(0,T))$ such that the unique solution $y\in C([0,T];H_0^1(\Omega))\cap C^1([0,T];L^2(\Omega))$ of

$$\left\{\begin{array}{ll} y_{tt}-\Delta y=v_\omega \mathcal{X}_\omega, & \Omega\times(0,T),\\ y=0, & \partial\Omega\times(0,T),\\ (y(\cdot,0),y_t(\cdot,0))=(y^0,y^1), & \Omega, \end{array}\right. \tag{1}$$

satisfies

$$y(.,T)=y_t(.,T)=0,\quad \text{on}\quad \Omega. \tag{2}$$

y_t denotes the derivative of y with respect to t and $\mathcal{X}_\omega\in L^\infty(\Omega,\{0,1\})$ denotes the characteristic function of the subset ω. We introduce the set

$$V(y^0,y^1,T)=\{\omega\subset\Omega \text{ such that (2) holds}\} \tag{3}$$

which contains in particular Ω. Moreover, from [3] assuming $\Omega\in C^\infty(\mathbb{R}^2)$, any subset ω satisfying the geometric control condition in Ω (*"Every ray of geometric optics that propagates in Ω and is reflected on its boundary enters ω in time less than T"*) belongs to $V(y^0,y^1,T)$. On the other hand, if Ω is rectangular and T large enough (dependent of the diameter of $\Omega\backslash\omega$), then any domain ω is in $V(y^0,y^1,T)$ (see [12]).

The control problem formulated above is usually referred to as internal (or distributed) controllability problem. The controllability property may be obtained using the Hilbert Uniqueness Method (HUM) introduced by J.-L. Lions in [19], which reduces the problem to an optimal control one. Precisely, for any $\omega\in V(y^0,y^1,T)$, the unique control v_ω of minimal L^2-norm (refereed as the HUM control in the sequel) may be obtained by minimizing the functional $\mathcal{J}:L^2(\Omega)\times H^{-1}(\Omega)\to\mathbb{R}$ defined by

$$\mathcal{J}(\phi^0,\phi^1)=\frac{1}{2}\int_\omega\int_0^T\phi^2(\boldsymbol{x},t)dtdx+<\phi_t(\cdot,0),y^0>_{H^{-1}(\Omega),H_0^1(\Omega)}-\int_\Omega y^1\phi(\cdot,0)dx, \tag{4}$$

where $<\cdot,\cdot>_{H^{-1},H_0^1}$ denotes the duality product between $H^{-1}(\Omega)$ and $H_0^1(\Omega)$ and ϕ the solution of the adjoint homogeneous system

$$\left\{\begin{array}{ll} \phi_{tt}-\Delta\phi=0, & \Omega\times(0,T),\\ \phi=0, & \partial\Omega\times(0,T),\\ (\phi(\cdot,T),\phi_t(\cdot,T))=(\phi^0,\phi^1), & \Omega. \end{array}\right. \tag{5}$$

This provides the following characterization of the HUM-control (see [19], chapter 7).

THEOREM 1.1. *Given any $(y^0,y^1)\in H_0^1(\Omega)\times L^2(\Omega)$, $T>0$ and $\omega\in V(y^0,y^1,T)$, the functional $\mathcal{J}$ has a unique minimizer $(\hat{\phi}^0,\hat{\phi}^1)\in L^2(\Omega)\times H^{-1}(\Omega)$. If $\hat{\phi}$ is the corresponding solution of (5) with initial data $(\hat{\phi}^0,\hat{\phi}^1)$ then $v=-\hat{\phi}\mathcal{X}_\omega$ is the control of (1) with minimal L^2-norm.*

This result is based on the following observation or observability inequality (leading to the coercivity of $\mathcal{J}$ in $L^2(\Omega)\times H^{-1}(\Omega)$): there exists a constant $C_{T,\omega}>0$ function of T and ω (called the observability constant) such that

$$||(\phi^0,\phi^1)||^2_{L^2(\Omega)\times H^{-1}(\Omega)}\leq C_{T,\omega}\int_\omega\int_0^T\phi^2(\boldsymbol{x},t)dt\,dx \tag{6}$$

for all $(\phi^0, \phi^1) \in L^2(\Omega) \times H^{-1}(\Omega)$. Therefore, from a practical viewpoint, ω being fixed in $V(y^0, y^1, T)$, such a control is determined by solving the linear system

$$\Lambda(\phi^0, \phi^1) = (y^1, -y^0) \quad \text{in} \quad \Omega, \tag{7}$$

where the isomorphism Λ from $L^2(\Omega) \times H^{-1}(\Omega)$ onto $H_0^1(\Omega) \times L^2(\Omega)$ is defined by $\Lambda(\phi^0, \phi^1) := (\psi_t(0), -\psi(0))$ and ψ is the unique solution of

$$\begin{cases} \psi_{tt} - \Delta\psi = -\phi\mathcal{X}_\omega, & \Omega \times (0,T), \\ \psi = 0, & \partial\Omega \times (0,T), \\ (\psi(\cdot,T), \psi_t(\cdot,T)) = (0,0), & \Omega. \end{cases} \tag{8}$$

The HUM control is then $v_\omega = -\phi\mathcal{X}_\omega$ and $y = \psi$.

Related to the controllability problem (1)-(2), we consider for any $(y^0, y^1) \in H_0^1(\Omega) \times L^2(\Omega)$ and $T > 0$ fixed, the following problem :

$$(\mathcal{P}_\omega) : \inf_{\omega \subset V_L(y^0,y^1,T)} J(\mathcal{X}_\omega), \quad \text{where} \quad J(\mathcal{X}_\omega) = \frac{1}{2}||v_\omega||^2_{L^2(\omega\times(0,T))}, \tag{9}$$

and $V_L(y^0, y^1, T) = \{\omega \in V(y^0, y^1, T); |\omega| = L|\Omega|\}$ for some $L \in (0,1)$, which consists in finding the optimal location of ω in order to minimize the L^2-norm of the corresponding HUM control v_ω. The size restriction on ω will be justified in the sequel. This optimal shape design problem may be not well-posed in the sense that there is no solution in the class of characteristic function: the optimal subset ω may be composed of an arbitrarily large number of disjoints components. A sufficient condition for $(\mathcal{P}_\omega)$ to be well-posed is to restrict the number of disjoints components (we refer to the books [9] and [14] for a complete description in the static case).

In this work, we numerically solve the problem $(\mathcal{P}_\omega)$ and proceed as in [21] where the author considers a damped wave equation and optimizes the position of the damping zone in order to minimize the energy of the system at a given time $T > 0$. Since the control associated to the optimal solution ω is *a fortiori* a HUM control (that is of minimal $L^2(0,T)$ norm), $(\mathcal{P}_\omega)$ is reduced to find the optimal HUM control with respect to ω. In this way, we use the explicit characterization of v_ω in term of the solution ϕ of (5). To the knowledge of the author, the problem $(\mathcal{P}_\omega)$ has never been studied so far. In the similar context of the boundary controllability, it is worth to mention the work of Asch-Lebeau [2] where the relationships between the geometry of the domain, the geometry of the controlled boundary, and the energy of the control are dealt with. Moreover, in order to take into account the size restriction, we introduce a positive multiplier λ and then consider the problem:

$$\inf_{\omega \subset \Omega, \lambda \in \mathbb{R}^+} J_\lambda(\mathcal{X}_\omega) \quad \text{where} \quad J_\lambda(\mathcal{X}_\omega) = J(\mathcal{X}_\omega) + \lambda(||\mathcal{X}_\omega||_{L^1(\Omega)} - L|\Omega|). \tag{10}$$

The outline of the paper is as follows. In section 2, we first compute the variation of J_λ with respect to smooth variations of ω. This derivative expressed as a curvilinear integral on $\partial\omega \times (0,T)$ independently of any adjoint solution permits to define a descent direction and build a minimizing sequence of domains for J_λ. The corresponding gradient algorithm is presented in section 3 in the framework of the level set approach and is efficiently initialized by the topological derivative associated to J_λ. In section 4, we point out the sensibility of the controllability problem with respect to the numerical approximation, and then present an efficient and robust semi-discrete scheme in space to solve (7) (the resolution (analytical in time) is discussed in the appendix 8). In section 5, numerical experiments are detailed and discussed. Then, in section 6, we investigate whether or not the problem $(\mathcal{P}_\omega)$ is

well-posed by considering its convexification ($\mathcal{CP}_\omega$). Numerical examples are given and compared with those of section 5. Finally, we give some concluding remarks and perspectives in section 7. Results of this paper were partially announced in [22].

2. Shape and topological derivatives of J_λ

In order to solve the problem ($\mathcal{P}_\omega$) with a gradient descent procedure, we first compute explicitly the derivative of the functional J_λ with respect to smooth variations of ω (the so-called shape derivative). In this respect, we assume that $\omega \in C^1(\Omega)$, Ω being fixed in $\mathbb{R}^2$. Let $\eta \in \mathbb{R}^+$ and a vector field $\boldsymbol{\theta} \in (W^{1,\infty}(\Omega,\mathbb{R}))^2$, $\boldsymbol{\theta}_{|\partial\Omega} = 0$ and not vanishing on a neighborhood of $\partial\omega$. Smooth perturbation ω^η of ω are then defined by the transformation $\mathcal{F}^\eta : \boldsymbol{x} \to \boldsymbol{x} + \eta\boldsymbol{\theta}(\boldsymbol{x}) \in \Omega^\eta = \Omega$ such that $\omega^\eta = \mathcal{F}^\eta(\omega)$. The parameter η is arbitrarily small so that $\det(\nabla\mathcal{F}^\eta) > 0$ in Ω and $\omega^\eta \subset \Omega$.

Definition 2.1. *The derivative of the functional J_λ with respect to a variation of $\omega \subset \Omega$ in the direction $\boldsymbol{\theta}$ is defined as the Fréchet derivative in $(W^{1,\infty}(\Omega,\mathbb{R}))^2$ at 0 of the application $\eta \to J_\lambda(\mathcal{X}_{(Id+\eta\boldsymbol{\theta})(\omega)})$, i.e.*

$$J_\lambda(\mathcal{X}_{(Id+\eta\boldsymbol{\theta})(\omega)}) = J_\lambda(\mathcal{X}_\omega) + \eta\frac{\partial J_\lambda(\mathcal{X}_\omega)}{\partial\omega}\cdot\boldsymbol{\theta} + o(\eta). \tag{11}$$

It is worth to mention that the initial condition (y^0, y^1) is independent of ω and that the field $\boldsymbol{\theta}$ is time independent (since ω is time independent). We refer the reader to [9] for the methodology to compute the shape derivative. Using formal Taylor expansion (which may be rigorously justified), we obtain the following result:

THEOREM 2.2. *Let $\omega \in V(y^0, y^1, T)$ and v_ω be the HUM control for (1). If ω is of class $C^1(\Omega)$ and if $(y^0, y^1) \in (H^2(\Omega) \cap H_0^1(\Omega)) \times H_0^1(\Omega)$, then the first lagrangian derivative of J_λ with respect to ω exists and is given by the following expression:*

$$\frac{\partial J_\lambda(\mathcal{X}_\omega)}{\partial\omega}\cdot\boldsymbol{\theta} = \frac{1}{2}\int_\omega\int_0^T (2v_\omega V_\omega + v_\omega^2 div\boldsymbol{\theta})\,dtdx + \lambda\int_\omega div\boldsymbol{\theta}\,dx \tag{12}$$

where V_ω is the control of minimal $L^2(\omega\times(0,T))$-norm associated to the following system:

(13)
$$\begin{cases} Y_{tt} - \Delta Y - \nabla(div\boldsymbol{\theta}).\nabla y + div((\nabla\boldsymbol{\theta} + \nabla\boldsymbol{\theta}^T).\nabla y) = V_\omega\mathcal{X}_\omega, & \Omega\times(0,T),\\ Y = 0, & \partial\Omega\times(0,T),\\ (Y(\cdot,0), Y_t(\cdot,0)) = (\nabla y^0\cdot\boldsymbol{\theta}, \nabla y^1\cdot\boldsymbol{\theta}), & \Omega, \end{cases}$$

such that $Y(\cdot,T) = Y_t(\cdot,T) = 0$ in Ω.

The couple (Y, V_ω) is the first lagrangian derivative of (y, v_ω) and is as expected the solution of an exact controllability problem. Remark that the null controllability of (13) may be obtained from the Hilbert Uniqueness Method (see Theorem 2.6 page 423) since $(Y(\cdot,0), Y_t(\cdot,0)) \in H_0^1(\Omega)\times L^2(\Omega)$. In the sequel, we will use the following expression of the shape derivative in terms of a curvilinear integral on $\partial\omega$.

THEOREM 2.3. *Let $\omega \in V(y^0, y^1, T)$, v_ω the HUM control for (1) and $\boldsymbol{\nu}$ be the unit normal vector oriented toward the exterior of ω. If ω is of class $C^1(\Omega)$ and if $(y^0, y^1) \in (H^2(\Omega) \cap H_0^1(\Omega)) \times H_0^1(\Omega)$, then the derivative of J_λ with respect to ω is given by the following expression :*

$$\frac{\partial J_\lambda(\mathcal{X}_\omega)}{\partial\omega}\cdot\boldsymbol{\theta} = -\frac{1}{2}\int_{\partial\omega}\int_0^T v_\omega^2(\boldsymbol{x},t)dt\,\boldsymbol{\theta}\cdot\boldsymbol{\nu}\,d\sigma + \lambda\int_{\partial\omega}\boldsymbol{\theta}\cdot\boldsymbol{\nu}\,d\sigma \tag{14}$$

Proof of the Theorem 2.3. The expression (14) may be obtained from the relation (12) after several integrations by part with respect to $\boldsymbol{x}$ and t. We refer to [21] for an example of calculation in a similar context and to [9] for a general presentation. Simpler, we use the Cea's method [8] and introduce the Lagrangian

$$\begin{aligned}\mathcal{L}(\omega,\overline{\phi},\overline{\psi},\overline{p},\overline{q}) =& \frac{1}{2}\int_\omega\int_0^T \overline{\phi}^2\,dtdx\\ &-\int_\Omega\int_0^T \overline{\phi}'\overline{p}'\,dtdx+\int_\Omega[\,\overline{\phi}'\overline{p}\,]_0^T\,dx+\int_\Omega\int_0^T\nabla\overline{\phi}\cdot\nabla\overline{p}\,dtdx\\ &-\int_\Omega\int_0^T \overline{\psi}'\overline{q}'\,dtdx+\int_\Omega[\,\overline{\psi}'\overline{q}\,]_0^T\,dx+\int_\Omega\int_0^T\nabla\overline{\psi}\cdot\nabla\overline{q}\,dtdx\\ &+\int_\omega\int_0^T \overline{\phi}\,\overline{q}\,dtdx,\end{aligned}\tag{15}$$

for all $\overline{\psi},\overline{p}\in C([0,T];H^2(\Omega)\cap H_0^1(\Omega))\cap C^1([0,T];H_0^1(\Omega))$, $\overline{\phi},\overline{q}\in C([0,T];H_0^1(\Omega))\cap C^1([0,T];L^2(\Omega))$. $\mathcal{L}$ is chosen so that the optimality conditions $<\frac{\partial\mathcal{L}}{\partial\overline{p}}(\omega,\phi,\overline{\psi},\overline{p},q),p>=0$ and $<\frac{\partial\mathcal{L}}{\partial\overline{q}}(\omega,\overline{\phi},\psi,p,\overline{q}),q>=0$ lead for all p,q to respectively the weak formulations associated to ϕ and ψ solutions of (5)-(7)-(8):

$$-\int_\Omega\int_0^T \phi'\overline{p}'\,dtdx+\int_\Omega[\,\phi'\overline{p}\,]_0^T\,dx+\int_\Omega\int_0^T\nabla\phi\cdot\nabla\overline{p}\,dtdx=0\tag{16}$$

and

$$-\int_\Omega\int_0^T \psi'\overline{q}'\,dtdx+\int_\Omega[\,\psi'\overline{q}\,]_0^T\,dx+\int_\Omega\int_0^T\nabla\psi\cdot\nabla\overline{q}\,dtdx=-\int_\omega\int_0^T\phi\,\overline{q}\,dtdx.\tag{17}$$

We then write formally that

$$\begin{aligned}\frac{d\mathcal{L}}{d\omega}(\boldsymbol{\theta}) =& \frac{\partial}{\partial\omega}\mathcal{L}(\omega,\overline{\phi},\overline{\psi},\overline{p},\overline{q})\cdot\boldsymbol{\theta}+<\frac{\partial}{\partial\overline{\phi}}\mathcal{L}(\omega,\overline{\phi},\overline{\psi},\overline{p},\overline{q}),\frac{\partial\overline{\phi}}{\partial\omega}\cdot\boldsymbol{\theta}>\\ &+<\frac{\partial}{\partial\overline{\psi}}\mathcal{L}(\omega,\overline{\phi},\overline{\psi},\overline{p},\overline{q}),\frac{\partial\overline{\psi}}{\partial\omega}\cdot\boldsymbol{\theta}>+<\frac{\partial}{\partial\overline{p}}\mathcal{L}(\omega,\overline{\phi},\overline{\psi},\overline{p},\overline{q}),\frac{\partial\overline{p}}{\partial\omega}\cdot\boldsymbol{\theta}>\\ &+<\frac{\partial}{\partial\overline{q}}\mathcal{L}(\omega,\overline{\phi},\overline{\psi},\overline{p},\overline{q}),\frac{\partial\overline{q}}{\partial\omega}\cdot\boldsymbol{\theta}>\end{aligned}\tag{18}$$

where $\frac{\partial\overline{p}}{\partial\omega}\cdot\boldsymbol{\theta}$ denotes the first derivative of $\overline{p}$ in the direction $\boldsymbol{\theta}$. The variables $\overline{\phi},\overline{\psi},\overline{p}$ and $\overline{q}$ being independent of ω, the first term in (18) is

$$\frac{\partial}{\partial\omega}\mathcal{L}(\omega,\overline{\phi},\overline{\psi},\overline{p},\overline{q})(\boldsymbol{\theta})=\frac{1}{2}\int_\omega\int_0^T\mathrm{div}(\overline{\phi}^2\boldsymbol{\theta})\,dtdx+\int_\omega\int_0^T\mathrm{div}(\overline{\phi}\,\overline{p}\,\boldsymbol{\theta})\,dtdx.\tag{19}$$

In addition, by definition of $\mathcal{L}$, the fourth and fifth terms are equal to zero for $(\overline{\phi},\overline{\psi})=(\phi,\psi)$ solution of (5)-(8). Let us then determine the adjoint functions p and q such that the following equality

$$<\frac{\partial}{\partial\phi}\mathcal{L}(\omega,\overline{\phi},\overline{\psi},p,q),\frac{\partial\overline{\phi}}{\partial\omega}\cdot\boldsymbol{\theta}>+<\frac{\partial}{\partial\psi}\mathcal{L}(\omega,\overline{\phi},\overline{\psi},p,q),\frac{\partial\overline{\psi}}{\partial\omega}\cdot\boldsymbol{\theta})>=0\tag{20}$$

holds for all $\overline{\phi}\in C([0,T];H_0^1(\Omega))\cap C^1([0,T];L^2(\Omega))$ and for all $\overline{\psi}\in C([0,T];H^2(\Omega)\cap H_0^1(\Omega))\cap C^1([0,T];H_0^1(\Omega))$. The interpretation of (20) implies that q is the unique solution in $C([0,T];H_0^1(\Omega))\cap C^1([0,T];L^2(\Omega))$ (the regularity of ϕ) of

$$\left\{\begin{array}{ll} q_{tt}-\Delta q=0, & \Omega\times(0,T),\\ q=0, & \partial\Omega\times(0,T),\\ (q(\cdot,0),q_t(\cdot,0))=(q^0,q^1), & \Omega,\end{array}\right.\tag{21}$$

where $(q^0, q^1) \in H_0^1(\Omega) \times L^2(\Omega)$ is such that the solution $p \in C([0,T]; H^2(\Omega) \cap H_0^1(\Omega)) \cap C^1([0,T]; H_0^1(\Omega))$ of

$$\left\{ \begin{array}{ll} p_{tt} - \Delta p = -(\phi + q)\mathcal{X}_\omega \equiv -F\mathcal{X}_\omega, & \Omega \times (0,T), \\ p = 0, & \partial\Omega \times (0,T), \\ (p(\cdot,T), p_t(\cdot,T)) = (\mathbf{0}, \mathbf{0}), & \Omega, \end{array} \right. \tag{22}$$

fulfills $(p(\cdot,0), p_t(\cdot,0)) = (\mathbf{0},\mathbf{0}) \in (H^2(\Omega) \cap H_0^1(\Omega)) \times H_0^1(\Omega)$! Equivalently, the function $F \equiv \phi + q$ fulfills the formulation

$$\left\{ \begin{array}{ll} F_{tt} - \Delta F = 0, & \Omega \times (0,T), \\ F = 0, & \partial\Omega \times (0,T), \\ (F(\cdot,0), F_t(\cdot,0) = (\phi^0 + q^0, \phi^1 + q^1), & \Omega, \end{array} \right. \tag{23}$$

where $(\phi^0 + q^0, \phi^1 + q^1)$ is such that $(p(\cdot,0), p_t(\cdot,0)) = (\mathbf{0},\mathbf{0})$ in Ω. The restriction $-F\mathcal{X}_\omega$ is then the control of minimal $L^2(\omega \times (0,T))$-norm which stabilizes at time T the functions $(F(\cdot,T), F_t(\cdot,T))$ starting from the initial state $(F(\cdot,0), F_t(\cdot,0)) = (\mathbf{0},\mathbf{0})$ (using the same argument than $-\phi\mathcal{X}_\omega$ for y and the reversibility in time of the system (22)). We then deduce that $F = 0$ in $\omega \times (0,T)$ and then on $\Omega \times (0,T)$ (by the Holmgren Theorem, see [19], Lemma 2.5 page 423). Consequently, $q = -\phi$ on $\Omega \times (0,T)$. Then, writing $J_0(\omega) = \mathcal{L}(\omega, \phi, \psi, p, q)$, we get from (19),

$$\frac{\partial J_0(\mathcal{X}_\omega)}{\partial \omega} \cdot \boldsymbol{\theta} = \frac{\partial}{\partial \omega}\mathcal{L}(\omega, \phi, \psi, p, q) \cdot \boldsymbol{\theta} = -\frac{1}{2}\int_\omega \int_0^T \mathrm{div}(\phi^2 \boldsymbol{\theta})\, dtdx \tag{24}$$

then the relation (14) assuming enough regularity on v_ω.

Remark 1.
- *As expected, the adjoint functions (p,q), dual of the first lagrangian derivatives $(\frac{\partial \phi}{\partial \omega}\cdot\boldsymbol{\theta}, \frac{\partial \psi}{\partial \omega}\cdot\boldsymbol{\theta})$ solve an exact (adjoint) control problem. Moreover, we remark that the shape derivative (14) is expressed independently of the adjoint solution (p,q). This is due to the minimal $L^2(0,T)$-norm property of the HUM control v_ω.*
- *It results from the relation (14) that the inclusion $\omega_1 \subset \omega_2 \subset \Omega$ implies $J_0(\omega_2) \leq J_0(\omega_1)$. In particular, for $\lambda = 0$, the optimal domain is $\omega = \Omega \in V(y^0, y^1, T)$. This justifies the introduction of the subset $V_L(y^0, y^1, T)$ in the formulation of $(\mathcal{P}_\omega)$. Similarly, for any fixed ω, the functional J_0 is a decreasing function of T (see* [2]*).*

In a very similar way, one may obtain easily the so-called topological derivative (see [25]) associated to J_λ. The adjoint method introduced in [10] leads to the following result (used in section 5).

THEOREM 2.4. *For any $\boldsymbol{x_0} \in \Omega$ and ρ such that $D(\boldsymbol{x_0}, \rho) \equiv \{\boldsymbol{x} \in \mathbb{R}^2, dist(\boldsymbol{x}, \boldsymbol{x_0}) \leq \rho\} \subset \Omega$, the functional J_λ associated to $\Omega \backslash D(\boldsymbol{x_0}, \rho)$ may be expressed as follows :*

$$J_\lambda(\mathcal{X}_{\Omega\backslash D(\boldsymbol{x_0},\rho)}) = J_\lambda(\mathcal{X}_\Omega) + \pi\rho^2\left(\frac{1}{2}\int_0^T v_\Omega^2(\boldsymbol{x_0}, t)dt - \lambda\right) + o(\rho^2) \tag{25}$$

in term only of the HUM control v_Ω associated to (1) with $\omega = \Omega$. The term factor of ρ^2 is called the topological derivative of J_λ at the point $\boldsymbol{x_0}$.

3. Minimization of J_λ by the level set approach

Thanks to the previous computations, we are now in position to apply a gradient descent method for the minimization of the objective function J_λ with respect to

the position and shape of ω. Precisely, from the relation (14), a descent direction is found by defining on $\partial\omega$, the vector field $\boldsymbol{\theta}$ as follows :

$$\boldsymbol{\theta} = \left(\frac{1}{2}\int_0^T v_\omega^2(\boldsymbol{x},t)dt - \lambda\right)\boldsymbol{\nu} \equiv j_\lambda(v_\omega)\boldsymbol{\nu} \quad on \quad \partial\omega, \tag{26}$$

and then we update the shape ω as $\omega^\eta = (Id + \eta\boldsymbol{\theta})(\omega)$ (we recall that ω is in $C^1(\Omega)$). The parameter $\eta > 0$ denotes a descent step small enough so that the following formal relation

$$J_\lambda(\mathcal{X}_{\omega^\eta}) = J_\lambda(\mathcal{X}_\omega) - \eta\int_{\partial\omega}(j_\lambda(v_\omega)^2)d\sigma + O(\eta^2) \tag{27}$$

guarantees the decrease of J_λ. It is crucial to remark that since $\omega \in V(y^0, y^1, T)$, this will imply that $\omega^\eta \in V(y^0, y^1, T)$. This method can be implemented in the Lagrangian framework: it suffices to mesh the domains ω, $\Omega\backslash\omega$ and then to advect the mesh according to the descent direction $\boldsymbol{\theta}$ defined on $\partial\omega$ by (26). This imposes to mesh the moving interface $\partial\omega$. In addition, the re-meshing of the domain at each step may produce a costly method. Finally, the change of topology of $\partial\omega$ is quite difficult to handle with this approach. In this respect, following recent works ([1, 5, 28]) dedicated to optimal shape design, we adopt an Eulerian approach and we use a level-set method to capture the shape ω on a fixed mesh. Let us briefly recall the main aspects of this method. The level set approach (see [26, 27] for a survey) consists in giving a description of the evolving interface $\partial\omega$ which is independent of the discretizing mesh on Ω. We define the level-set function ψ in Ω such that

$$\psi(\boldsymbol{x}) \leq 0 \quad \boldsymbol{x} \in \omega, \quad \psi(\boldsymbol{x}) = 0 \quad \boldsymbol{x} \in \partial\omega, \quad \psi(\boldsymbol{x}) \geq 0 \quad \boldsymbol{x} \in \Omega\backslash\omega. \tag{28}$$

Therefore, the evolving interface $\partial\omega$ is characterized by

$$\partial\omega = \{\boldsymbol{x}(\tau) \in \Omega \text{ such that } \psi(\boldsymbol{x}(\tau),\tau) = 0\}, \tag{29}$$

where τ designs a pseudo-time variable, increasing with time, that may be the real time, a load factor or in our case, the iterations of a given algorithm. Denoting by $\boldsymbol{F}$ the speed in the outward normal direction, such that $\frac{d\boldsymbol{x}(\tau)}{d\tau}.\boldsymbol{\nu} = \boldsymbol{F}(\boldsymbol{x}(\tau))$ where $\boldsymbol{\nu} = \nabla\psi/|\nabla\psi|$, the differentiation in τ of (29) then leads to the following nonlinear Hamilton-Jacobi equation of first order for ψ:

$$\frac{\partial\psi}{\partial\tau}(\boldsymbol{x},\tau) + \boldsymbol{F}(\boldsymbol{x},\tau)|\nabla\psi(\boldsymbol{x},\tau)| = 0, \quad \text{given} \quad \psi(\boldsymbol{x},\tau=0). \tag{30}$$

Assuming that the shape $\partial\omega$ evolves in pseudo-time τ with the normal velocity $\boldsymbol{F} = -j_\lambda(v_\omega)\boldsymbol{\nu}$ as proposed in (26), the transport of the level set function ψ is therefore equivalent to moving the boundary of ω (the zero level-set of ψ) along the descent gradient direction $-\partial J_\lambda/\partial\omega$. Consequently, the partial differential system to solve is

$$\begin{cases} \dfrac{\partial\psi}{\partial\tau} - j_\lambda(v_\omega)|\nabla\psi| = 0 \quad \text{in} \quad \Omega\times(0,\infty), \\ \psi(.,\tau=0) = \psi_0 \quad \text{in} \quad \Omega, \qquad \psi = \psi_0 > 0 \quad \text{on} \quad \partial\Omega\times(0,\infty). \end{cases} \tag{31}$$

We further impose ψ to be constant and positive on Ω in order to ensure that $\partial\omega \cap \partial\Omega = \emptyset$. Finally, because of its advection, the level-set function may become too flat or too steep yielding either large errors in the location of its zero level or large errors in the evaluation of its gradient by finite differences. Therefore, a

standard trick (see [5]) consists in replacing the level-set ψ at the pseudo-time τ_0 by the regularized one, solution of the following problem

$$\begin{cases} \dfrac{\partial\tilde{\psi}}{\partial\tau} + \text{sign}(\psi(\tau_0))(|\nabla\tilde{\psi}| - 1) = 0 \quad \text{in} \quad \Omega\times(0,\infty), \\ \tilde{\psi}(.,\tau=0) = \psi(\tau_0) \quad \text{in} \quad \Omega, \qquad \tilde{\psi} = \psi(\tau_0) \quad \text{on} \quad \partial\Omega\times(0,\infty) \end{cases} \tag{32}$$

admitting as a stationary solution the signed distance to the initial interface $\{\psi(\boldsymbol{x},\tau_0) = 0\}$.

Remark 2. *The behavior of the level set function is therefore strongly linked with the asymptotic behavior in the pseudo-time variable τ of the system (31). This question seems difficult and largely open. Some results in this direction exist under some very restrictive assumptions on $\boldsymbol{F}$ (see* [4] *and the references therein).*

Consequently, the descent algorithm to solve numerically the problem $(\mathcal{P}_\omega)$ in the framework of the level set approach may be structured as follows : $\Omega \in \mathbb{R}^2$, $(y^0, y^1) \in H_0^1(\Omega)\times L^2(\Omega)$, $T > 0$ and $\varepsilon_1 << 1$ be given,

(i) Meshing once for all of the fixed domain Ω. Initialization of the level-set ψ^0 corresponding to an initial guess $\omega^0 \in V_L(y^0, y^1, T)$;

(ii) For $k \geq 0$, iteration until convergence (i.e. $\mid J_\lambda(\mathcal{X}_{\omega^{k+1}}) - J_\lambda(\mathcal{X}_{\omega^k}) \mid \leq \varepsilon_1 J_\lambda(\mathcal{X}_{\omega^0})$) as follows:
- Computation of the HUM control v_{ω^k} associated to the domain ω^k. v_{ω^k} is obtained by solving the linear system (7) with a conjugate gradient algorithm.
- Computation on Ω of the integrand $j_\lambda(v_{\omega^k})$ according to the relation (14).
- Deformation of the shape by solving the transport Hamilton-Jacobi system (31). The new domain ω^{k+1} is characterized by the level-set function ψ^{k+1} solution of (31) after a pseudo-time step $\Delta\tau^k$ starting from the initial condition ψ^k with velocity $-j_\lambda(v_{\omega^k})$. The pseudo-time step $\Delta\tau^k$ is chosen according to the stability condition (40).

(iii) From time to time, for stability reasons, we re-initialize the level-set function ψ by solving (32).

At each iteration, the Lagrange multiplier $\lambda = \lambda^k$ is chosen so that the area of ω remains constant: $||\mathcal{X}_{\omega^k}||_{L^1(\Omega)} - ||\mathcal{X}_{\omega^{k+1}}||_{L^1(\Omega)} = 0\ \forall k \geq 0$. From the relation $\omega^{k+1} = (I + \eta\boldsymbol{\theta^k})\omega^k$, we obtain

$$||\mathcal{X}_{\omega^{k+1}}||_{L^1(\Omega)} - ||\mathcal{X}_{\omega^k}||_{L^1(\Omega)} = \eta\int_{\omega^k} div(\boldsymbol{\theta^k})dx + \eta^2\int_{\omega^k} det(\nabla\boldsymbol{\theta^k})dx. \tag{33}$$

Then, if we neglect the term factor of η^2 in (33), we deduce from (26) that

$$\lambda^k = \frac{1}{2}\int_{\omega^k} div\Big(\int_0^T v_{\omega^k}^2(\boldsymbol{x},t)\,dt\,\boldsymbol{\nu^k}\Big)dx \Big/ \int_{\omega^k} div(\boldsymbol{\nu^k})\,dx. \tag{34}$$

We remind that the normal $\boldsymbol{\nu^k}$ is extended to the whole domain Ω as follows : $\boldsymbol{\nu^k} = \nabla\psi^k/|\nabla\psi^k|$. Similarly, if the term of order η^2 is not neglected, then λ^k is the root of a polynomial of degree two.

Furthermore, the topological derivative (25) permits to initialize efficiently the domain ω^0. It suffices to compute the HUM control v_Ω corresponding to $\omega = \Omega$. This gives the distribution of the function $\boldsymbol{x} \to 1/2\int_0^T v_\Omega^2(\boldsymbol{x},t)dt$ on the domain Ω.

Then, the domain ω^0 is defined as follows

$$\omega^0 = \{\boldsymbol{x} \in \Omega, \frac{1}{2}\int_0^T v_\Omega^2(\boldsymbol{x},t)dt - \lambda > 0\} \tag{35}$$

where λ is chosen so that the area $||\mathcal{X}_{\omega^0}||_{L^1(\Omega)}$ of ω^0 be equal $L|\Omega|$. The level set function ψ^0, negative in ω^0, is then $\psi^0(\boldsymbol{x}) = \lambda - 1/2\int_0^T v_\Omega^2(\boldsymbol{x},t)dt$ for all $\boldsymbol{x}$ in Ω. Numerical illustrations are given in section 5.

4. Numerical Approximation

The main part of the algorithm is the computation of the HUM control associated to ω. It is well-known that such a problem is extremely sensitive to the numerical approximation. We briefly describe in this section a recent, robust and efficient method to compute numerically this control (detailed in the appendix 8).

4.1. Numerical approximation of the HUM control - Introduction of additional vanishing terms. Since the pioneering work of Glowinski-Li-Lions [11], the numerical approximation of the HUM control is known to be extremely sensitive with respect to the parameters of approximation (we refer to [29] for a review on this subject). For simplicity, let us take $\Omega = (0,1)^2$ and choose to approximate the wave system (1) by a semi-discrete finite difference scheme. Let us consider $N \in \mathbb{N}$, $h = 1/(N+1)$ and a uniform grid $(x_{1,i}, x_{2,j})_{(i,j=0,\dots,N+1)}$ of Ω. Let us denote by $\boldsymbol{v_h}$ the control vector of the finite dimensional system

$$\begin{cases} (\boldsymbol{y_h})_{tt} - \boldsymbol{\Delta_h}\boldsymbol{y_h} = \boldsymbol{v_h}\mathcal{X}_\omega, & \Omega \times (0,T), \\ \boldsymbol{y_h} = 0, & \partial\Omega \times (0,T), \\ (\boldsymbol{y_h}(0), (\boldsymbol{y_h})_t(0)) = (\boldsymbol{y_h^0}, \boldsymbol{y_h^1}), & \Omega, \end{cases} \tag{36}$$

such that $\boldsymbol{y_h}(T) = (\boldsymbol{y_h})_t(T) = 0$ on Ω. $\boldsymbol{\Delta_h}$ designates a consistent finite difference approximation of the operator Δ. Following [11], the control $\boldsymbol{v_h}$ of minimal l^2-norm may be obtained by solving the linear system $\boldsymbol{\Lambda_h}(\boldsymbol{\phi_h^0}, \boldsymbol{\phi_h^1}) = (\boldsymbol{y_h^1}, \boldsymbol{y_1^0})$ - semi discrete version of (7)- using a conjugate gradient algorithm. $\boldsymbol{\Lambda_h}$ designates the corresponding discrete HUM matrix. Let us note $P(\boldsymbol{v_h})$ the piecewise linear function on Ω such that $(P(\boldsymbol{v_h}))(x_{1,i}, x_{2,j}) = (v_h)_{i,j}, i,j = 0,...,N+1$. Numerical simulations ([7, 20]) highlight that the behavior of $e_h = ||v - P(\boldsymbol{v_h})||_{L^2(\omega\times(0,T))}$ with respect to the parameter of discretization h crucially depends on the approximation $\boldsymbol{\Delta_h}$ of Δ. For instance, if the centered five points approximation is used for $\boldsymbol{\Delta_h}$, then the error e_h blows up exponentially with $1/h$. This implies a wrong approximation of the descent direction $j_\lambda(v_\omega)$ and *a fortiori* a divergence of the descent algorithm of the section 3 ! This non commuting property between exact controllability and numerical approximation is due to the spurious high frequency oscillations generated by the discrete dynamics (36). These spurious oscillations propagate with a group velocity of order h and can not be controlled in a uniform (with respect to h) time T. In practice, we observe that the conditioning number of $\boldsymbol{\Lambda_h}$ behaves like $O(e^{1/h})$ which implies a divergence of the conjugate gradient algorithm (for h small enough). In order to restore the uniform convergence of the discrete control (and therefore expect a convergence of the level function $\boldsymbol{\psi_h^k}$ - approximation of ψ^k (see next section) - with respect to k), it is necessary to increase the group velocity of the high frequencies component. An efficient remedy recently introduced in [7, 23] consists in considering the approximation (using standard finite difference or finite

element method) of the so-called viscous wave equation

$$(I + \frac{h^2}{4}\partial_x^2)(I + \frac{h^2}{4}\partial_y^2)y_{tt} - \Delta y = v\mathcal{X}_\omega, \quad \Omega \times (0,T), \tag{37}$$

consistent with (1) and which group velocity is uniformly (with respect to h) bounded by below for all the components. Using a Fourier analysis [20] or a semi-discrete multiplier technique [7], one may obtain the following result.

THEOREM 4.1. *The semi-discrete scheme associated to (37) is uniformly controllable with respect to h. In addition, if $(P(\boldsymbol{y_h^0}), P(\boldsymbol{y_h^1}))$ converges strongly toward (y^0, y^1) in $H_0^1(\Omega) \times L^2(\Omega)$ as h goes to 0, then the corresponding control $\boldsymbol{v_h}$ of minimal l^2-norm is such that $\lim_{h\to 0} ||P(\boldsymbol{v_h}) - v||_{L^2(\omega\times(0,T))} = 0$.*

The conditioning number $\text{cond}(\boldsymbol{\Lambda_h})$ of the discrete HUM matrix associated to this modified scheme is of order h^{-2}. In practice, this modification leads to a very fast convergence of the conjugate gradient algorithm, obtained after few iterations independent of the value of h (see [23] for detailed numerical simulations). Moreover, on the square domain where the eigenvalues and eigenvectors of the discrete scheme are known, the control $\boldsymbol{v_h}$ may be solved exactly in time via a spectral method. This is detailed in the appendix 8. For general domain, a time discretization is necessary and we refer to [23] for uniformly controllable (with respect to both h and Δt) full discrete approximation of (1).

4.2. Resolution of the Hamilton-Jacobi equation. Let us now briefly consider the resolution of the non-linear Hamilton-Jacobi equation (31). We introduce a parameter $\Delta\tau > 0$ and note by $\boldsymbol{\psi_h^k}$ the approximation of the function ψ at the point $(x_{1,i}, x_{2,j}), i, j = 0, ..., N+1$ and at the pseudo-time $\tau = k\Delta\tau$. We note $\boldsymbol{j_{\lambda h}} = (j_\lambda)_{i,j}$ the approximation of $j_\lambda(v_\omega^k)$ such that

$$\boldsymbol{j_{\lambda h}} = \frac{1}{2}\int_0^T (\boldsymbol{v_h})^2 dt - \lambda. \tag{38}$$

The hyperbolic system (31) is then solved using an explicit weighted essentially non-oscillatory scheme of order one in pseudo-time τ and of order two in space (see [26, 27] for a complete description):

$$\frac{\boldsymbol{\psi_h^{k+1}} - \boldsymbol{\psi_h^k}}{\Delta\tau} + \left(\max(-\boldsymbol{j_{\lambda h}}(v_{\omega^k}), 0)\nabla_k^+ + \min(-\boldsymbol{j_{\lambda h}}(v_{\omega^k}), 0)\nabla_k^-\right) = 0, \quad k > 0 \tag{39}$$

where (∇_k^+, ∇_k^-) designates forward and upward approximation of $|\nabla\psi^k|$. This explicit scheme is stable under the condition $\Delta\tau \leq h/\max_\Omega|\boldsymbol{j_{\lambda h}}(v_{\omega^k})|$. In order that the pseudo-time step $\Delta\tau$ decreases with respect to the iterations k, we consider the following pseudo-time step

$$\Delta\tau^k = \min\left(1, \max_\Omega|\boldsymbol{j_{\lambda h}}(v_{\omega^k})|\right)\frac{h}{\max_\Omega|\boldsymbol{j_{\lambda h}}(v_{\omega^k})|} \quad (\leq \Delta\tau^{k-1}), \quad \forall k > 0. \tag{40}$$

Remark 3. *The upwind scheme (39) is motivated by the propagation of information through characteristics in the first order hyperbolic equation (30). Very interestingly with respect to the discussion of the previous section, this scheme may be replaced by usual centered finite differences ones, provided the addition of an artificial viscosity term (see* [26]*) (namely the approximation of $\psi_\tau + F|\nabla\psi| = h\Delta\psi$ instead of (30)).*

5. Numerical experiments - First part

In this section, we present some numerical experiments in order to evaluate the efficiency of the previous algorithm to find local minima of the functional J_λ. Since the computation of the HUM control (via the resolution of (7)) is more expensive in CPU time than the resolution of the Hamilton-Jacobi system (31), we perform two explicit pseudo-time steps of (31) after each resolution of (1). During these steps, we perform two re-initialization of the level set function by solving (32). Moreover, the numerical results are obtained with $\varepsilon_1 = 10^{-6}$ (see the algorithm) and $h = 1/60$. The test value on the residual for the conjugate gradient algorithm used to solve (7) is $\epsilon = 10^{-6}$: this implies that the energy associated to (1) fulfills at time T the relation $E_h(T) \leq 10^{-6} E_h(0)$. We recall that the energy at time t is defined by $E(t, y) = 1/2 \int_\Omega (|y'|^2 + |\nabla y|^2) dx$. For simplicity, all the computations are performed on the unit square.

Let us then consider the following regular initial condition, on $\Omega = (0, 1)^2$

$$y^0(\boldsymbol{x}) = e^{-100((x_1-0.3)^2+(x_2-0.3)^2)} \mathcal{X}_\Omega(\boldsymbol{x}); \quad y^1(\boldsymbol{x}) = 0. \tag{41}$$

This initial condition is clearly of finite state. Therefore, from [12], the exact controllability property holds for any domain $\omega \subset \Omega$ provided that T is large enough depending on the diameter of $\Omega \backslash \omega$.

We take $T = 3$ and $L = 1/10$. Let us first use the relation (25). The iso-values of the function $\boldsymbol{x} \to 1/2 \int_0^T v_\Omega^2(\boldsymbol{x}, t) dt$ are depicted on figure 1-left. The function reachs a global maximum at the point $(0.3, 0.3)$ where y^0 is concentrated and many local maxima, notably at the point $(0.7, 0.7)$. Figure 1-right depicts the boundary of the domain ω^0 defined by $\omega^0 = \{\boldsymbol{x} \in \Omega, -1/2 \int_0^T v_\Omega^2(\boldsymbol{x}, t) dt + \lambda \leq 0\}$ where λ is determined so that $|\omega^0| = L|\Omega|$. We obtain $\lambda \approx 1.5$. As expected, the prediction ω^0 is composed of several disjoint components, mainly distributed on the first diagonal of Ω. We note $\psi^0_{opt}(\boldsymbol{x}) = -1/2 \int_0^T v_\Omega^2(\boldsymbol{x}, t) dt + 1.5$ the corresponding function, negative on ω^0, we may choose to initialize the level set algorithm. Moreover, for $T = 3$, we check that ω^0 belongs to $V(y^0, y^1, T)$: we obtain $J(\mathcal{X}_{\omega^0}) \approx 5.30$.

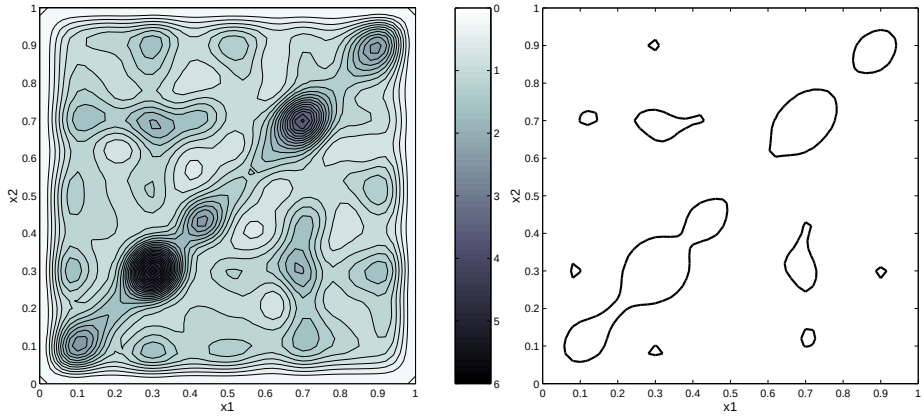

FIGURE 1. $T = 3$ - Left: Iso-values of $\int_0^T v_\Omega^2(\boldsymbol{x}, t) dt$ on Ω - Right : $\partial\omega^0 = \{\boldsymbol{x} \in \Omega, 1/2 \int_0^T (v_\Omega(\boldsymbol{x}, t))^2 dt - \lambda = 0\}$, $\lambda \approx 1.5$, $\omega^0 \in V(y^0, y^1, T)$.

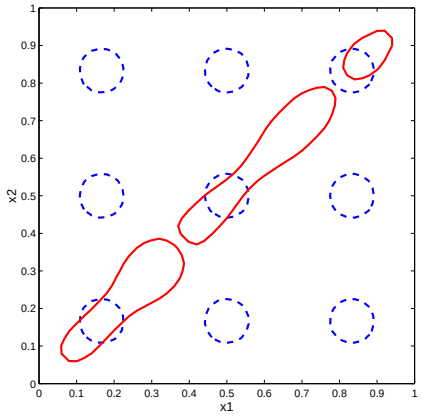

FIGURE 2. $T = 3$ - Zeros of the initial level set $\psi^0_{p=3}$ and of the limit one $\psi^{lim}_{p=3}$- $J(\mathcal{X}_{\omega^0_3}) \approx 12.50$, $J(\mathcal{X}_{\omega^{lim}_3}) \approx 6.42$.

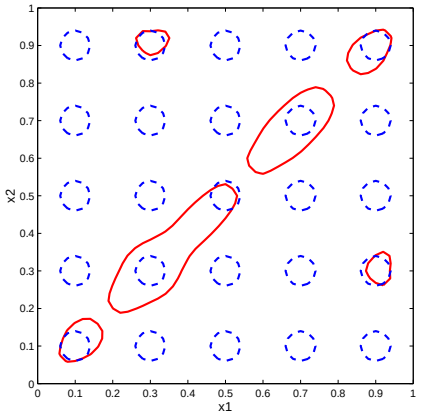

FIGURE 3. $T = 3$ - Zeros of the initial level set $\psi^0_{p=3}$ and of the limit one $\psi^{lim}_{p=5}$- $J(\mathcal{X}_{\omega^0_5}) \approx 8.47$, $J(\mathcal{X}_{\omega^{lim}_5}) \approx 5.07$.

We now compare the result of the level set algorithm initialized either by ψ^0_{opt} or by functions of the type $\psi^0_p(\boldsymbol{x}) = C_p - |\sin(p\pi x_1)\sin(p\pi x_2)|$, $p \in \mathbb{N}$ and $C_p \in \mathbb{R}^+$ such that $||\mathcal{X}_{\psi^0_p \leq 0}||_{L^1(\Omega)} = L|\Omega|$. The corresponding ω^0_p is composed of $p \times p$ C^1-disjoints components uniformly distributed on Ω. Figures 2 and 3 depict the zeros of the limit level set function ψ^{lim}_p corresponding to $p = 3$ and $p = 5$ respectively. We check numerically that for $T = 3$, there exist controls supported on $\omega^0_{p=3}$ and $\omega^0_{p=5}$ which stabilize the system (1), i.e. $\omega^0_{p=3}, \omega^0_{p=5} \in V(y^0, y^1, T)$. In both case, the convergence is obtained in less than 300 iterations. We observe that $p = 3$ and $p = 5$ produce two different results highlighting the dependence of the initialization on the limit and the existence of local minima. As expected, the value $p = 5$ produces a better cost value: for $p = 3$, we obtain $J(\mathcal{X}_{\omega^0_3}) \approx 12.50$ and $J(\mathcal{X}_{\omega^{lim}_3}) \approx 6.42$ while for $p = 5$, we obtain $J(\mathcal{X}_{\omega^0_5}) \approx 8.47$ and $J(\mathcal{X}_{\omega^{lim}_5}) \approx 5.07$. We remark that these limit domains are similar to the prediction obtained from the relation (25) highlighting also the efficiency of the topological derivative. Due to the symmetries of y^0, the domain is concentrated on the first diagonal of the unit square Ω. Moreover, for $T = 3$ and $p = 3$, Figure 4 depicts the corresponding evolution of $J_0(\omega^k)$. The oscillations are due to the fact that $|\omega^k|$ is not strictly constant but oscillates around $L|\Omega|$. On the same figure, the evolution of the corresponding ratio

$$\frac{||\phi^0_{\omega^k}||^2_{L^2(\Omega)} + ||\phi^1_{\omega^k}||^2_{H^{-1}(\Omega)}}{\int_{\omega^k}\int_0^T (\phi_{\omega^k}(\boldsymbol{x},t))^2 dt\, dx} \tag{42}$$

which appears in (6), is depicted. We remind that $||\phi^1_{\omega^k}||_{H^{-1}(\Omega)} = ||v||_{H^1_0(\Omega)}$ where v is solution of $-\Delta v = \phi^1_{\omega^k}$ in Ω and $v = 0$ on $\partial\Omega$. The fact that this ratio decreases implies that the domain ω^{k+1} leads to a better estimation of the norm $||(\phi^0, \phi^1)||_{L^2 \times H^{-1}}$ than ω^k. Thus, by minimizing the L^2-norm of the exact control with respect to its support, we increase the observability/controllability character of the wave system (we remind that the constant $C_{T,\omega}$ in (6) is arbitrarily large if (1) is not exactly controllable with the couple (ω, T)). As a matter of fact, since

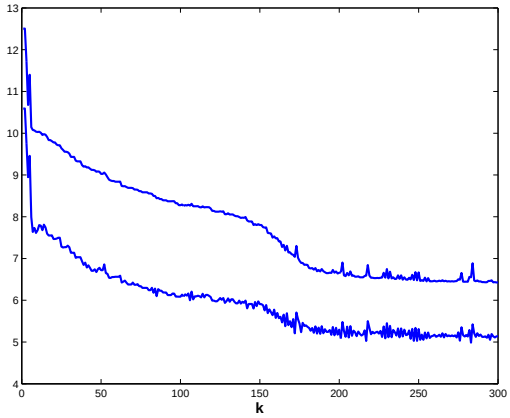

FIGURE 4. $T = 3$- Evolution of $J_0(\omega^k)$ (top) and corresponding ratio (42) (bottom) vs. k.

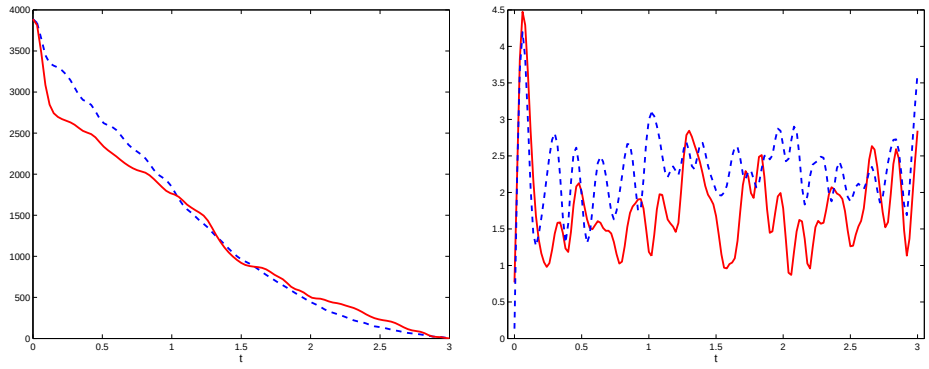

FIGURE 5. $T = 3$ - Energy $E(y,t)$ of the system (left) and $||v_\omega||_{L^2(\omega)}$ (right) vs. t- $E(y,T)/E(y,0) \approx 2.40 \times 10^{-6}$ corresponding to the initial level set function $\psi^0_{p=3}$ $(--)$ and to the limit one $\psi^{lim}_{p=3}$ $(-)$.

$J(\mathcal{X}_{\omega^{k+1}}) \leq J(\mathcal{X}_{\omega^k})$, if (1) is exactly controllable for (ω^k, T) at the iteration k, then (1) remains exactly controllable for $(\omega^{k+1}, T) = ((I + \eta\boldsymbol{\theta^k})(\omega^k), T)$.

Figures 5 represents the energy $E(y,t)$ of the wave system (left) and the $L^2(\omega \times (0,T))$-norm of v_ω with respect to time, associated to the initial domain $\omega^0_{p=3}$ (dashed curve) and to the limit one $\omega^{lim}_{p=3}$ (continuous curve).

Furthermore, the optimal location clearly depends on the value of T. Figures 6 depicts the iso-values of the topological derivative (left) and the boundary (right) of initial prediction of ω^0 obtained for instance for $T = 10$, slightly different from the result obtained with $T = 3$. We numerically check that $\omega^0 \in V(y^0, y^1, T)$ (the conjugate gradient algorithm converges) and we obtain $J(\mathcal{X}_{\omega^0}) \approx 2.41$.

On the other hand, for small values of T, a direct use of the relation (25) may be inappropriate to initialize efficiently the support of the control. We recall that this relation is valid for a couple (ω, T) for which system (1) is exactly controllable and may be applied if the area $|\omega|$ is small. These two conditions are incompatible if T is small enough. Thus, for $T = 1$, (25) leads to an initial prediction ω^0

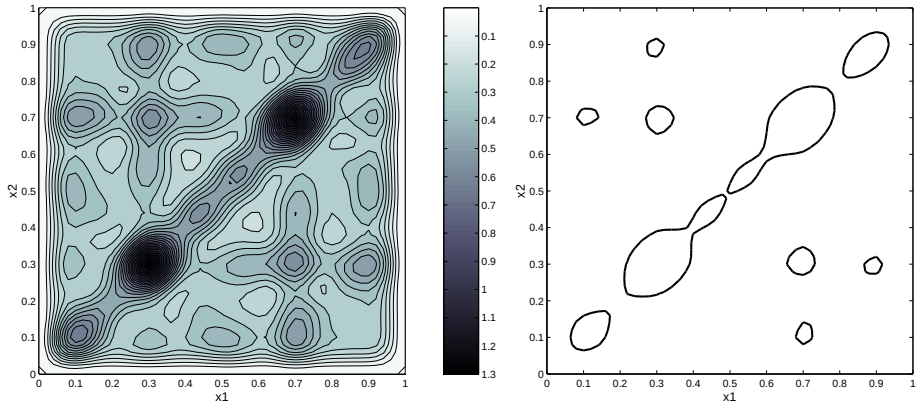

FIGURE 6. $T = 10$ - Left: Iso-values of $1/2 \int_0^T v_\Omega^2(\boldsymbol{x}, t)dt$ on Ω - Right : $\partial\omega^0 \equiv \{\boldsymbol{x} \in \Omega, 1/2 \int_0^T (v_\Omega(\boldsymbol{x}, t))^2 dt - \lambda = 0\}$, $\lambda \approx 0.82$, $\omega^0 \in V(y^0, y^1, T)$.

mainly concentrated around the point of coordinates $(x_1, x_2) = (0.3, 0.3)$ (see the iso-values of the function $1/2 \int_0^T v_\Omega(\boldsymbol{x}, t)^2 dt$ on Figure 7-left and the boundary $\partial\omega^0$ of the prediction ω^0 on the figure 7-right). We observe numerically that $\omega^0 \notin V(y^0, y^1, T)$ (the CG-algorithm diverges). On the other hand, Figure 8 depicts the zeros of the limit level set function $\psi_{p=5}^{lim}$ initialized with $\psi_{p=5}^0$ corresponding to a uniformly distributed $\omega_{p=5}^0$ composed of 25 components on Ω for which (1) is exactly controllable ($\omega_{p=5}^0 \in V(y^0, y^1, T = 1)$). In agreement with the figure 7-right, we observe that the main part of the domain $\omega_{p=5}^{lim}$ is located around the point $(0.3, 0.3)$. The domain contains also many small components distributed (symmetrically) on the whole domain which permit to observe the system at the time $T = 1$.

More generally, remark that the method we present permits to find numerically the exact HUM control of (1) associated to an arbitrarily small value of T distributed on ω_T (dependent on T) of arbitrarily small Lebesgue measure $|\omega_T|$! One may conjecture that the number of disjoints components of the optimal domain ω_T is an increasing function of T^{-1}. In the next section, additional simulations are presented.

6. Relaxation of the problem $(\mathcal{P}_\omega)$

We investigate in this section whether or not the problem $(\mathcal{P}_\omega)$ may be not well-posed: is there exist an initial condition $(y^0, y^1) \in H_0^1(\Omega) \times L^2(\Omega)$ for which the infimum cost function is not reached in the set of characteristic function ? In such a case, the optimal sub-domain ω is composed of an arbitrarily large number of disjoint components and the original problem is thus non well-posed. The numerical detection of this phenomenon with the level set approach may be done as follows: (i) consider an initial level set function ψ_p of the type $\psi_p(\boldsymbol{x}) = C_p - |\sin(p\pi x_1)\sin(p\pi x_2)|$, $C_p \in]0, 1[$ associated to a domain ω_p composed of $p^2 \in \mathbb{N}$ disjoint components uniformly distributed in Ω; (ii) compute with the algorithm described above the limit level set function ψ_p^{lim} associated to a domain ω_p^{lim}; (iii) count the number $\sharp\omega_p^{lim}$ of disjoint components of ω_p^{lim}. Then, the variation of the function $p \to \sharp\omega_p^{lim}$ permits to detect the possible ill-posedness of $(\mathcal{P}_\omega)$. However, for large values of p, this method requires very small values of h and cannot be

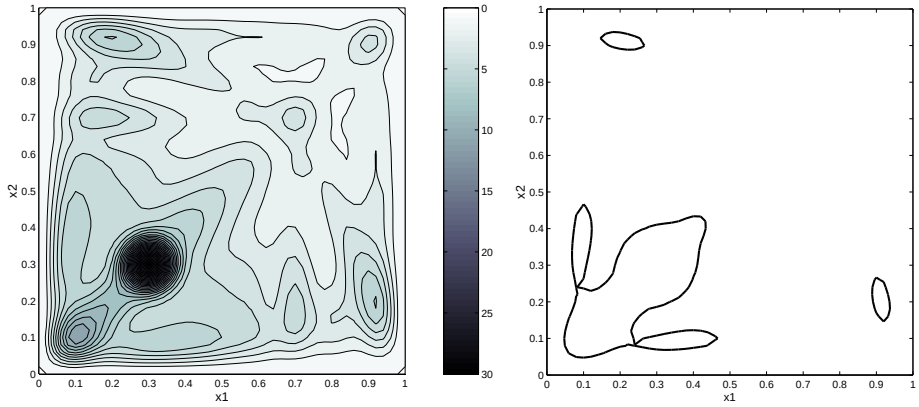

FIGURE 7. $T = 1$ - Left: Iso-values of $1/2 \int_0^T v_\Omega^2(\boldsymbol{x}, t)dt$ on Ω - Right : $\partial\omega^0 = \{\boldsymbol{x} \in \Omega, 1/2 \int_0^T (v_\Omega(\boldsymbol{x}, t))^2 dt - \lambda = 0\}$, $\lambda \approx 5.30$, $\omega^0 \notin V(y^0, y^1, T)$.

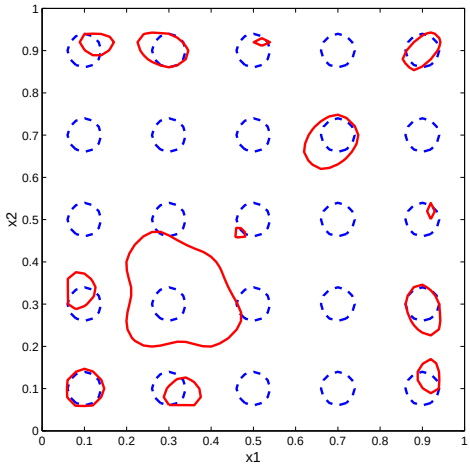

FIGURE 8. Limit of $\partial\omega_k = \{\boldsymbol{x} \in \Omega, \psi_k(\boldsymbol{x}) = 0\}$ vs. k for $T = 1$ - $J(\mathcal{X}_{\omega^0_{p=5}}) \approx 29.321$, $J(\mathcal{X}_{\omega^{lim}_{p=5}}) \approx 15.314$.

used. Another method consists in replacing the set $L^\infty(\Omega, \{0, 1\})$ of characteristics function by it weak-$\star$ closure $L^\infty(\Omega, [0, 1])$ (or equivalently its convex envelop). We then define the convexified problem $(\mathcal{CP}_\omega)$ of $(\mathcal{P}_\omega)$ as follows :

(43)

$$(\mathcal{CP}_\omega) : \inf_{s \in L^\infty(\Omega;[0,1])} \overline{J}_\lambda(s) \quad \text{with} \quad \overline{J}_\lambda(s) = \frac{1}{2} \int_\Omega s(\boldsymbol{x}) \int_0^T v_s^2(\boldsymbol{x}, t)dtdx + \lambda \int_\Omega s(\boldsymbol{x})dx$$

where v_s (function of the density s) is such that sv_s is the HUM control of minimal $L^2(\Omega \times (0, T))$ norm associated to

(44)

$$\begin{cases} y_{tt} - \Delta y = s(\boldsymbol{x})v_s, & \Omega \times (0, T), \\ y = 0, & \partial\Omega \times (0, T), \\ (y(\cdot, 0), y_t(\cdot, 0)) = (y^0, y^1), & \Omega. \end{cases}$$

Once again, the multiplier λ is chosen so that $\int_\Omega s(\boldsymbol{x})dx = L|\Omega|$, relaxed version of the condition $|\omega| = L|\Omega|$. Thus, the optimal (topological) shape design problem $(\mathcal{P}_\omega)$ is replaced by a simpler *functional* optimal problem. It is easy to see that problem $(\mathcal{CP}_\omega)$ is well posed and admits solutions in $L^\infty(\Omega;[0,1])$. Moreover, problems $(\mathcal{CP}_\omega)$ and $(\mathcal{P}_\omega)$ both coincide if and only if the optimal density s for $(\mathcal{CP}_\omega)$ is a characteristic function. On the contrary, if the optimal density s takes value in $]0,1[$, this indicates that the original problem is ill-posed.

Similarly to problem $(\mathcal{P}_\omega)$, local minimal density may be obtained using a gradient descent method. For any $\eta \in \mathbb{R}^+$ and any $s_1 \in L^\infty(\Omega)$, we associate to the perturbation $s^\eta = s + \eta s_1$ the derivative of $\overline{J}_\lambda$ with respect to s in the direction s_1 as follows:

$$\frac{\partial \overline{J}_\lambda(s)}{\partial s} \cdot s_1 = \lim_{\eta \to 0} \frac{\overline{J}_\lambda(s+\eta s_1) - \overline{J}_\lambda(s)}{\eta} \tag{45}$$

and we obtain that :

THEOREM 6.1. *If $(y^0, y^1) \in (H^2(\Omega) \cap H_0^1(\Omega)) \times H_0^1(\Omega)$, then the derivative of $\overline{J}_\lambda$ with respect to s in the direction s_1 exists and takes the expression*

$$\frac{\partial \overline{J}_\lambda(s)}{\partial s} \cdot s_1 = \int_\Omega s_1(\boldsymbol{x}) \left(-\frac{1}{2} \int_0^T v_s^2(\boldsymbol{x},t)dt + \lambda \right) dx. \tag{46}$$

■

This permits to define the following descent direction :

$$s_1(\boldsymbol{x}) = \frac{1}{2} \int_0^T v_s^2(\boldsymbol{x},t)dx - \lambda, \quad \forall \boldsymbol{x} \in \Omega. \tag{47}$$

Consequently, for any function $\eta \in L^\infty(\Omega, \mathbb{R}^+)$ with $||\eta||_{L^\infty}$ small enough, we have $\overline{J}_\lambda(s+\eta s_1) \leq \overline{J}_\lambda(s)$. The multiplier λ is determined so that, for any function $\eta \in L^\infty(\Omega, \mathbb{R}^+)$ and $\eta \neq 0$, $||s+\eta s_1||_{L^1(\Omega)} = L|\Omega|$ leading to

$$\lambda = \frac{(\int_\Omega s(\boldsymbol{x})dx - L|\Omega|) - \int_\Omega \eta(\boldsymbol{x}) \int_0^T v_s^2(\boldsymbol{x},t)\, dtdx}{\int_\Omega \eta(\boldsymbol{x})dx}. \tag{48}$$

At last, the function η is chosen so that $s(\boldsymbol{x}) + \eta s_1(\boldsymbol{x}) \in [0,1]$ for all $\boldsymbol{x} \in \Omega$. A simple and efficient choice consists in taking $\eta = \varepsilon s(\boldsymbol{x})(1 - s(\boldsymbol{x}))$ for all $\boldsymbol{x} \in \Omega$ with ε a small real positive. Consequently, the descent algorithm which permits to solve the problem $(\mathcal{CP}_\omega)$ may be structured as follows : let $\Omega \in \mathbb{R}$, $(y^0, y^1) \in (H^2(\Omega) \cap H_0^1(\Omega)) \times H_0^1(\Omega)$, $L \in (0,1)$, $T > T(\Omega)$ and $\varepsilon < 1, \varepsilon_1 << 1$ be given:

- Initialization of the density function $s^0 \in L^\infty(\Omega;]0,1[)$;
- For $k \geq 0$, iteration until convergence (i.e. $|\overline{J}_0(s^{k+1}) - \overline{J}_0(s^k)| \leq \varepsilon_1 |\overline{J}_0(s^0)|$) as follows :
  - Computation of the HUM control $s^k v_{s^k}$ corresponding to $s = s^k$.
  - Computation of the descent direction s_1^k defined by (47) where the multiplier λ^k is defined by (48) with $\eta = \varepsilon s(1-s)$.
  - Update of the density function in Ω:

$$s^{k+1} = s^k + \varepsilon s^k (1 - s^k) s_1^k \tag{49}$$

with $\varepsilon \in \mathbb{R}^+$ small enough in order to ensure the decrease of the cost function and $s^{k+1} \in L^\infty(\Omega, [0,1])$.

We now complete the section 5 with additional simulations using this new approach. Once again, we consider the simple initial condition (41) and choose to

initialize the density s by $s^0(\boldsymbol{x}) = L = 1/10$ in Ω (so that $\int_\Omega s^0(\boldsymbol{x})dx = L|\Omega|$). We take $\varepsilon = 10^{-2}$ and $\varepsilon_1 = 10^{-6}$.

Figure 9 depicts the evolution with respect to k of the cost function $\overline{J}(s^k)$ and of the ratio

$$\frac{||\phi^0_{s^k}||^2_{L^2(\Omega)} + ||\phi^1_{s^k}||^2_{H^{-1}(\Omega)}}{\int_\Omega s^k(\boldsymbol{x}) \int_0^T (\phi_{s^k}(\boldsymbol{x},t))^2 dtdx}, \tag{50}$$

relaxed version of the ratio (42). Once again, this ratio is decreasing with respect to k. Figure 10 depicts the iso-value of the limit of the density s^k in Ω. First, we observe that this limit density is a characteristic function. Therefore, at least for these data, the problem $(\mathcal{CP}_\omega)$ coincides with $(\mathcal{P}_\omega)$ which is well-posed. Secondly, the method produces a similar limit domain than the level-set approach (see figures 2 and 3) and lead to a better value of the cost function: $\overline{J}(s^{lim}) \approx 4.95$.

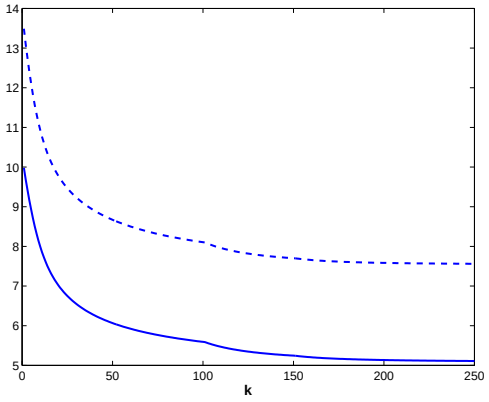

FIGURE 9. $T = 3$- $\overline{J}_0(s^k)$ (bottom) and corresponding ratio (50) (top) vs. k.

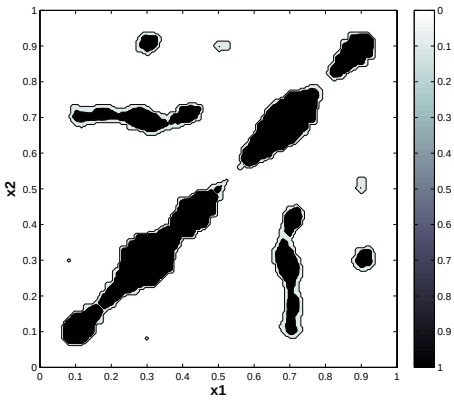

FIGURE 10. Iso-values of the limit density function s^{lim} for $T = 3$ initialized with $s^0 = L$ on $\Omega = (0,1)^2$.

Figures 11 represent the density limit s^{lim} corresponding to $T = 0.5$ and $T = 1$. Once again, the density limit belongs to $L^\infty(\Omega, \{0,1\})$ and provides a better value of the cost function than the level set approach (see Figure 8): for $T = 1$, we obtain $\overline{J}(s^{lim}) \approx 13.42$. As expected, in both cases, the main part of the optimal domain is concentrated around the point $(0.3, 0.3)$. For $T = 1$, the components are distributed (symmetrically) on the whole domain.

We have not been able to exhibit an initial condition $(y^0, y^1) \in (H^2(\Omega) \cap H^1_0(\Omega)) \times H^1_0(\Omega)$ (nor in $H^1_0(\Omega) \times L^2(\Omega)$) leading to a limit density s^{lim} such that $|\{\boldsymbol{x} \in \Omega, 0 < s(\boldsymbol{x}) < 1\}| > 0$. Therefore, we conjecture that the problem $(\mathcal{P}_\omega)$ is always well-posed: the infimum of J is reached for a domain composed of a finite number of disjoints components. The introduction of the relaxed problem $(\mathcal{CP}_\omega)$ is however not useless: on the practical viewpoint, the algorithm described in this section appears more simple and less sensitive to numerical approximation than the algorithm based on the level set methodology. It avoids the resolution of Hamilton-Jacobi equation and provides a more regular decrease of the cost function.

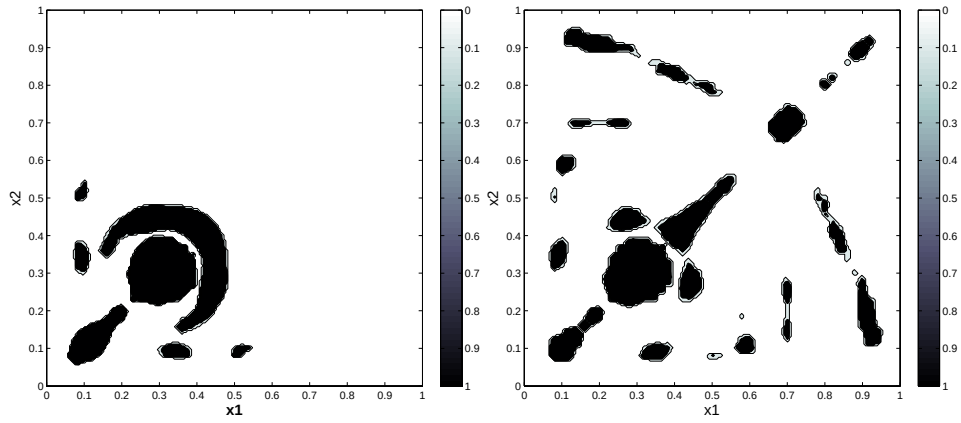

FIGURE 11. Limit density function s^{lim} for $T = 0.5$ (left) and $T = 1$ (right) initialized with $s^0 \equiv L$ on $\Omega = (0, 1)$.

7. Concluding remarks

We have presented a numerical method to obtain the optimal position of the distributed control for the 2-D wave equation. The method is based on an iterative descent algorithm of first order which requires at each iteration the computation of a HUM control v_ω and the computation of a descent direction $\boldsymbol{\theta}$. The function v_ω is obtained using recent, efficient and robust scheme mixing conjugate gradient algorithm and finite difference approach. The field $\boldsymbol{\theta}$, expressed independently of any adjoint control function, is obtained directly from v_ω. These two aspects explain the interest of the approach. In addition, the numerical experiments illustrate the potential of the topological derivative to initialize the algorithm. Moreover, as expected, the optimal domain depends on the initial condition and also on the time T. It is interesting to notice that the method is able to find the HUM control distributed on ω (of arbitrarily small measure $|\omega|$) which drives to rest the system (1) after an arbitrarily small time $T > 0$. We may conjecture that for small values of T, the optimal domain is composed of several disjoints components distributed on the whole domain Ω so that all the wave components be observed by ω in a time lower or equal than T. Furthermore, from the numerical resolution of the relaxed problem $(\mathcal{CP}_\omega)$ of $(\mathcal{P}_\omega)$, we may conjecture that the original problem is well-posed in the class of characteristic functions. Following [24] in a similar context, it is worth to investigate theoretically whether or not $(\mathcal{CP}_\omega)$ and $(\mathcal{P}_\omega)$ always coincide for any initial condition in $H_0^1(\Omega) \times L^2(\Omega)$ and value of T. It would be also interesting to extend this work to more general systems like the elasticity one, and also to treat the boundary case. Finally, the treatment of time-dependent domains $(\omega(t))_{t\in[0,T]}$ seems open and challenging.

8. Appendix : Exact resolution in time

The aim of this appendix is to detail the exact resolution in time of the semi-discrete wave systems in ϕ (5) and ψ (8) which appear at each iteration of the conjugate gradient algorithm used to solve the linear system (7) (accordingly to the HUM method). The wave equations (5) and (8) are solved using a viscous finite difference scheme similar to (37). Let us first present the exact resolution in

time of the semi-discrete system associated to (5):

$$\begin{cases} (I+\frac{h^2}{4}\partial^2_{x,h})(I+\frac{h^2}{4}\partial^2_{y,h})(\boldsymbol{\phi_h})_{tt}-\boldsymbol{\Delta_h}\boldsymbol{\phi_h}=0, & \Omega\times(0,T),\\ \boldsymbol{\phi_h}=0, & \partial\Omega\times(0,T),\\ (\boldsymbol{\phi_h}(0),(\boldsymbol{\phi_h})_t(0)=(\boldsymbol{\phi^0_h},\boldsymbol{\phi^1_h}), & \Omega, \end{cases} \tag{51}$$

that we may write in the following vectorial form :

$$\begin{cases} M\boldsymbol{\phi_h}''(t)+K_h\boldsymbol{\phi_h}(t)=0, \quad t\in(0,T),\\ (\boldsymbol{\phi_h}(0),\boldsymbol{\phi'_h}(0))=(\boldsymbol{\phi^0_h},\boldsymbol{\phi^1_h}) \end{cases} \tag{52}$$

where M and $K_h \in \mathcal{M}_{N^2\times N^2}(\mathbb{R})$ designate the mass and stiffness matrices respectively. These matrices are tri-diagonal bloc matrices, symmetric and definite positive. Moreover, let us designate by $V_h, D_h \in \mathcal{M}_{N^2\times N^2}(\mathbb{R})$ the eigenvector and eigenvalue matrix respectively of $M^{-1}K_h$ such that $K_hV_h = MV_hD_h$. The matrix $D_h = (\lambda_k)_{1\le k\le N^2}$ is diagonal, with

$$\lambda_k = \frac{4}{h^2}\frac{\sin^2(\frac{m\pi h}{2})+\frac{\sin^2(n\pi h)}{2}}{\cos^2(\frac{m\pi h}{2})\cos^2(\frac{n\pi h}{2})}, \quad k=m\times N+n, \quad m,n=1,...,N \tag{53}$$

whereas the matrix V_h is symmetric and orthonormal such that $V_h^2 = I_{N^2\times N^2}$. The eigenvectors corresponding to λ_k is $V_k = (\sin(pm\pi h)\sin(qn\pi h))_{p,q=1,...,N} \in \mathcal{M}_{N^2\times 1}(\mathbb{R})$. Therefore, the solution $\boldsymbol{\phi_h}(t) = (\phi_i(t))_{(1\le i\le N^2)}$ is

$$\phi_i(t) = \sum_{k=1}^{N^2} V_{ik}\left(a_k\cos(\sqrt{\lambda_k}t)+\frac{b_k}{\sqrt{\lambda_k}}\sin(\sqrt{\lambda_k}t)\right), \quad 1\le i\le N^2, t\ge 0 \tag{54}$$

where $(\boldsymbol{a_h},\boldsymbol{b_h}) = (V_h^{-1}\boldsymbol{\phi^0_h}, V_h^{-1}\boldsymbol{\phi^1_h})$ and $\boldsymbol{a_h} = (a_k)_{(1\le k\le N^2)}$, $\boldsymbol{b_h} = (b_k)_{(1\le k\le N^2)}$. Similarly, the semi-discretization of (8) takes the following form

$$\begin{cases} M(\boldsymbol{\psi_h})_{tt}(t)+K_h\boldsymbol{\psi_h}(t)=-\mathcal{X}_{\omega_h}\boldsymbol{\phi_h}(t), \quad t\in(0,T),\\ (\boldsymbol{\psi_h}(T),\boldsymbol{\psi'_h}(T))=(\mathbf{0},\mathbf{0}). \end{cases} \tag{55}$$

Let A the diagonal matrix in $\mathcal{M}_{N^2\times N^2}$ associated to $-\mathcal{X}_{\omega_h}$. It follows that the new variable $\boldsymbol{z_h}(t) = V_h^{-1}\boldsymbol{\psi_h}(t)$ is solution of

$$\begin{cases} \boldsymbol{z''_h}(t)+D_h\boldsymbol{z_h}(t)=(MV_h)^{-1}A\boldsymbol{\phi_h}(t), \quad t\in(0,T),\\ (\boldsymbol{z_h}(T),\boldsymbol{z'_h}(T))=(\mathbf{0},\mathbf{0}). \end{cases} \tag{56}$$

Then, introducing the matrix $P = (MV_h)^{-1}$, the j-th component of the vector $\boldsymbol{z_h}$ is solution of the ordinary differential equation

$$z_j''(t)+\lambda_j z_j(t) = \Big(PA\boldsymbol{\phi_h}(t)\Big)_j, \quad t\ge 0, \quad 1\le j\le N^2. \tag{57}$$

Using (54), the right hand term is

$$\begin{aligned} \Big(PA\boldsymbol{\phi_h}(t)\Big)_j &= \sum_{1\le k,l\le N^2} P_{jk}A_{kl}\phi_l(t)\\ &= \sum_{1\le k,l,p\le N^2} P_{jk}A_{kl}V_{lp}\left(a_p\cos(\sqrt{\lambda_p}t)+\frac{b_p}{\sqrt{\lambda_p}}\sin(\sqrt{\lambda_p}t)\right). \end{aligned} \tag{58}$$

Consequently, the component z_j is solution of the following system

(59)
$$z_j''(t)+\lambda_j z_j(t)=\sum_{1\le p\le N^2}\mathcal{B}_{jp}\left(a_p\cos(\sqrt{\lambda_p}t)+\frac{b_p}{\sqrt{\lambda_p}}\sin(\sqrt{\lambda_p}t)\right),\quad 1\le j\le N^2$$

where $\mathcal{B}=PAV_h$. Some computations lead to

(60)
$$\begin{aligned}z_j(t)=&C_1^j\cos(\sqrt{\lambda_j}t)+C_2^j\sin(\sqrt{\lambda_j}t)\\&+\sum_{1\le p\le N^2,\lambda_p\neq\lambda_j}\frac{\mathcal{B}_{jp}}{\lambda_j-\lambda_p}\left(a_p\cos(\sqrt{\lambda_p}t)+\frac{b_p}{\sqrt{\lambda_p}}\sin(\sqrt{\lambda_p}t)\right)\\&+\frac{1}{2}\sum_{1\le p\le N^2,\lambda_p=\lambda_j}\frac{\mathcal{B}_{jp}}{\lambda_p}\left((a_p-b_pt)\cos(\sqrt{\lambda_p}t)+a_p\sqrt{\lambda_p}t\sin(\sqrt{\lambda_p}t)\right)\\\equiv&C_1^j\cos(\sqrt{\lambda_j}t)+C_2^j\sin(\sqrt{\lambda_j}t)+F_j(t).\end{aligned}$$

We then use the condition at time T in (56) to fixe the constants C_1^j and C_2^j, for $1\le j\le N^2$;

(61)
$$\begin{aligned}C_1^j&=-\cos(\sqrt{\lambda_j}T)F_j(T)+\frac{\sin(\sqrt{\lambda_j}T)}{\sqrt{\lambda_j}}F_j'(T),\\C_2^j&=-\sin(\sqrt{\lambda_j}T)F_j(T)-\frac{\cos(\sqrt{\lambda_j}T)}{\sqrt{\lambda_j}}F_j'(T).\end{aligned}$$

Finally, we obtain the vector $\boldsymbol{\psi_h}(t)=V_h\boldsymbol{z_h}(t)$ for all $t\in(0,T)$. Then, making $t=0$ in (60), we obtain

(62)
$$z_j(0)=C_1^j+\sum_{1\le p\le N^2,\lambda_p\neq\lambda_j}\frac{\mathcal{B}_{jp}}{\lambda_j-\lambda_p}a_p+\frac{1}{2}\sum_{1\le p\le N^2,\lambda_p=\lambda_j}\frac{\mathcal{B}_{jp}}{\lambda_p}a_p$$

and a similar relation for $z_j'(0)$. This provides the explicit linear relation between the initial condition $(\boldsymbol{\phi_h^0},\boldsymbol{\phi_h^1})=(V_h\boldsymbol{a_h},V_h\boldsymbol{b_h})$ and $(\boldsymbol{\psi_h}(0),\boldsymbol{\psi_h'}(0))=(V_h\boldsymbol{z_h}(0),V_h\boldsymbol{z_h'}(0))=(\boldsymbol{y_h^0},\boldsymbol{y_h^1})$. The linear system $\boldsymbol{\Lambda_h}(\boldsymbol{\phi_h^0},\boldsymbol{\phi_h^1}):=(\boldsymbol{y_h^0},\boldsymbol{y_h^1})$ is then efficiently solved using a conjugate gradient algorithm initialized by $(\boldsymbol{\phi_h^0},\boldsymbol{\phi_h^1})=(\boldsymbol{0},\boldsymbol{0})$ (see [11, 20, 23]).

Remark 4. *The computation of $P=(MV_h)^{-1}$ is straightforward. From $M^{-1}=V_hD_MV_h^{-1}$ and $V_h^{-1}=V_h$, the matrix P is simply $P=(D_M)^{-1}V_h$ where D_M is the diagonal matrix composed of the (analytically known) eigenvalues of M.* ■

References

[1] Allaire G., Jouve F., Toader A.M., *Structural optimization using sensitivity analysis and level-set methods*, J. Comp. Phys. **194(1)**, 363-393 (2004).

[2] Asch M., Lebeau G., *Geometrical aspects of exact controllability for the wave equation - A numerical study*, Esaim : Cocv, **3**, 163-212 (1998).

[3] Bardos C., Lebeau G., Rauch J., *Sharp sufficient conditions for the observation, control and stabilization from the boundary*, SIAM J. Control and Opt., **30**, 1024-1065 (1992).

[4] Barles G., Sougadinis P.E., *On the large time behavior of solutions of Hamilton-Jacobi equations*, SIAM J. Math. Anal., **31(4)**, 925-939 (2000).

[5] Burger M., Osher S.J., *A survey on level set methods for inverse problems and optimal design*, European Journal of Applied Mathematics, **16(2)**, 263-301 (2005).

[6] Cagnol J., Zolesio J.P., *Shape derivative in the wave equation with Dirichlet boundary condition*, J. Diff. Eq **158**, 175-210, (1999).

[7] Castro C., Micu S., Münch A., *Numerical approximation of the boundary control of the 2-D wave equation with mixed finite elements.*, To appear in IMA Numerical Analysis.

[8] Cea J., *Conception optimale ou identification de formes, calcul rapide de la dérivée directionnelle de la fonction coût*, Math. Model. Num. Anal., **20(3)**, 371-402 (1986).

[9] Delfour M.C., Zolesio J.P., *Shapes and Geometries - Analysis, Differential Calculus and Optimization*, Advances in Design and Control, Siam, (2001).
[10] Garreau S., Guillaume P., Masmoudi M., *The topological asymptotic for PDE systems : the elasticity case*, SIAM J. Control Optim, **39(6)**, 1756-1778 (2001).
[11] Glowinski R., Li C.H., Lions J-L., *A numerical approach to the exact boundary controllability of the wave equation (I). Dirichlet controls: Description of the numerical methods*, Int. J. Numer. Methods. Eng., **27(3)**, 623-636 (1989).
[12] Haraux A., *A generalized internal control for the wave equation in a rectangle.*, J. Math. Anal. Appl. , **153**, 190-216 (1990).
[13] Hebrard P., Henrot A., *Optimal shape and position of the actuators for the stabilization of a string*, Systems and control letters, **48**, 199-209 (2003).
[14] Henrot A., Pierre M., *Variation et optimisation de formes : une analyse géométrique*, Mathématiques et Applications 48, Springer, (2005).
[15] Kapitonov B., Raupp M, *Simultaneous exact control of piezoelectric systems in multilayered media*, Comput. Appl. Math. **22** 249-277, (2003).
[16] Khludnev, A. M.; Sokolowski, J., *Modelling and control in solid mechanics.* International Series of Numerical Mathematics, **122.** Birkhuser Verlag, Basel, 1997.
[17] Komornik V., *Exact controllability and Stabilization - The multiplier method*, J. Wiley and Masson (1994).
[18] Lagnese, J.E. *Recent progress and open problems in control of multi-link elastic structures*, Contemp. Math., 161-175, (1996)
[19] Lions J.L., *Contrôlabilité exacte, stabilisation et perturbations de systèmes distribués, Tome 1*, Masson, RMA 8, Paris (1988).
[20] Münch A., *A uniformly controllable and implicit scheme for the 1-D wave equation*, Mathematical Modelling and Numerical Analysis **39(2)**, 377-418, (2005).
[21] Münch A., *Optimal internal stabilization of a damped wave equation by a level set approach*, Prépublication du laboratoire de Mathématiques de Besançon, 2005/1. (downlable at www-math.univ-fcomte.fr/amunch/research.htm).
[22] Münch A., *A shape optimal design problem related to the exact controllability of the 2-D wave equation*, C.R.Acad. Sci. Paris Série I, **343(3)**, 213-218, (2006)
[23] Münch A., *An implicit scheme uniformly controllable for the 2-D wave equation*, To appear in J. Sci. Comput.
[24] Münch A., Pedregal P., Periago F., *Optimal design of the damping set for the stabilization of the wave equation*, J. Diff. Eq. , **231(1)**, 331-358, (2006).
[25] Sokolowski J., Zochowski A., *On the topological derivative in shape optimization*, SIAM J. Control Optim., **37(4)**, 1251-1272 (1999).
[26] Osher S.J., Fedkiw R., *Level set methods and dynamics implicit surfaces*, Applied Mathematics Sciences, Springer-Verlag, **153**, (2002).
[27] Sethian J.A., *Level set methods: Evolving interfaces in geometry, fluid mechanics, computer vision, and materials science*, Cambridge University Press, (1996).
[28] Wang M.Y., Wang X., Guo D., *A level set method for structural topology optimization*, Computat. Methods. Appl. Mech. Engrg. **192**, 227-246, (2003).
[29] Zuazua E., *Propagation, Observation, Control and Numerical Approximation of Waves approximated by finite difference methods*, SIAM Review, **47(2)**, 197-243, (2005).

Laboratoire de Mathématiques de Besançon, UMR CNRS 6623, Université de Franche-Comte, 16 route de Gray 25030 Besançon cedex, France.
E-mail: arnaud.munch@univ-fcomte.fr
URL: http://www-math.univ-fcomte.fr/amunch/